The Conserved DNA Binding Protein WhiA Influences Chromosome Segregation in Bacillus subtilis

Bohorquez, L.C.; Surdova, K.; Jonker, M.J.; Hamoen, L.W.

DOI
10.1128/JB.00633-17

Publication date
2018

Document Version
Final published version

Published in
Journal of Bacteriology

AMERICAN SOCIETY FOR MICROBIOLOGY | Journal of Bacteriology®

RESEARCH ARTICLE

The Conserved DNA Binding Protein WhiA Influences Chromosome Segregation in *Bacillus subtilis*

Laura C. Bohorquez,[a] Katarina Surdova,[b]* Martijs J. Jonker,[c] Leendert W. Hamoen[a,b]

[a]Swammerdam Institute for Life Sciences, University of Amsterdam, Amsterdam, The Netherlands

[b]Centre for Bacterial Cell Biology, Institute for Cell and Molecular Biosciences, Newcastle University, Newcastle upon Tyne, United Kingdom

[c]RNA Biology and Applied Bioinformatics Research Group, Swammerdam Institute for Life Sciences, University of Amsterdam, Amsterdam, The Netherlands

ABSTRACT The DNA binding protein WhiA is conserved in Gram-positive bacteria and is present in the genetically simple cell wall-lacking mycoplasmas. The protein shows homology to eukaryotic homing endonucleases but lacks nuclease activity. WhiA was first characterized in streptomycetes, where it regulates the expression of key differentiation genes, including the cell division gene *ftsZ*, which is essential for sporulation. For *Bacillus subtilis*, it was shown that WhiA is essential when certain cell division genes are deleted. However, in *B. subtilis*, WhiA is not required for sporulation, and it does not seem to function as a transcription factor, despite its DNA binding activity. The exact function of *B. subtilis* WhiA remains elusive. We noticed that *whiA* mutants show an increased space between their nucleoids, and here, we describe the results of fluorescence microscopy, genetic, and transcriptional experiments to further investigate this phenomenon. It appeared that the deletion of *whiA* is synthetic lethal when either the DNA replication and segregation regulator ParB or the DNA replication inhibitor YabA is absent. However, WhiA does not seem to affect replication initiation. We found that a Δ*whiA* mutant is highly sensitive for DNA-damaging agents. Further tests revealed that the deletion of *parAB* induces the SOS response, including the cell division inhibitor YneA. When *yneA* was inactivated, the viability of the synthetic lethal Δ*whiA* Δ*parAB* mutant was restored. However, the nucleoid segregation phenotype remained. These findings underline the importance of WhiA for cell division and indicate that the protein also plays a role in DNA segregation.

IMPORTANCE The conserved WhiA protein family can be found in most Gram-positive bacteria, including the genetically simple cell wall-lacking mycoplasmas, and these proteins play a role in cell division. WhiA has some homology with eukaryotic homing endonucleases but lacks nuclease activity. Because of its DNA binding activity, it is assumed that the protein functions as a transcription factor, but this is not the case in the model system *B. subtilis*. The function of this protein in *B. subtilis* remains unclear. We noticed that a *whiA* mutant has a mild chromosome segregation defect. Further studies of this phenomenon provided new support for a functional role of WhiA in cell division and indicated that the protein is required for normal chromosome segregation.

KEYWORDS *Bacillus subtilis*, RecA, WhiA, YneA, cell division, chromosome segregation

The protein WhiA is present in most Gram-positive bacteria, including the genetically simple cell wall-lacking mycoplasmas. WhiA was first characterized in *Streptomyces* species. In these bacteria, FtsZ is induced at the onset of sporulation, leading to the

Received 17 October 2017 **Accepted** 22 January 2018

Accepted manuscript posted online 29 January 2018

Citation Bohorquez LC, Surdova K, Jonker MJ, Hamoen LW. 2018. The conserved DNA binding protein WhiA influences chromosome segregation in *Bacillus subtilis*. J Bacteriol 200:e00633-17. https://doi.org/10.1128/JB.00633-17.

Editor Tina M. Henkin, Ohio State University

Address correspondence to Leendert W. Hamoen, l.w.hamoen@uva.nl.

* Present address: Katarina Surdova, Hruskova 26, Bratislava, Slovakia.

L.C.B. and K.S. contributed equally to this article.

synthesis of septa that divide the tips of aerial hyphae into prespore compartments. Mutations in *whiA* prevent the induction of FtsZ and block sporulation (1–4). WhiA binds DNA and functions as a transcription activator of *ftsZ* and other differentiation genes in *Streptomyces* spp., and recently, it has been shown to regulate *ftsZ* in *Corynebacterium glutamicum* as well (4, 5).

WhiA proteins show some homology to eukaryotic homing endonucleases, and the crystal structure of WhiA from *Thermotoga maritima* reveals a bipartite structure in which a degenerate N-terminal LAGLIDADG homing endonuclease domain is tethered to a C-terminal helix-turn-helix domain. The N-terminal domain has lost residues critical for metal binding and catalysis, and the protein does not show any nuclease activity (6). How exactly WhiA regulates transcription is not yet clear.

In *Bacillus subtilis*, WhiA is essential for growth when certain cell division genes are deleted (7). Cell division begins with the polymerization of FtsZ at midcell into a ring-like structure, the so-called Z-ring. Several conserved proteins support the assembly of the Z-ring, including ZapA that cross-links FtsZ polymers and promotes polymer bundling (8, 9), and the transmembrane protein EzrA (10, 11). Z-ring assembly is regulated by the dynamic protein couple MinCD, which inhibits FtsZ polymerization close to cell poles and nascent septa (12–14), and the nucleoid occlusion protein Noc, which prevents the polymerization of FtsZ over the chromosome (15, 16). *B. subtilis* strains that lack either a functional *zapA*, *minCD*, *ezrA*, or *noc* gene still divide and grow normally. However, when *whiA* is also impaired in these mutants, cells become very filamentous and sick (7). This synthetic lethal cell division defect can be suppressed when *ugtP* is inactivated (7). UgtP transfers glucose from UDP-glucose to diacylglycerol, a key step in the synthesis of glycolipids. However, UgtP also suppresses FtsZ polymerization, and the protein functions as a metabolic sensor that couples nutritional availability to cell division (17).

B. subtilis WhiA binds DNA, but in contrast to streptomycetes and *C. glutamicum* WhiA, it does not influence the transcription of *ftsZ* or other cell division genes, and chromatin immunoprecipitation with microarray technology (ChIP-chip) experiments showed that the protein does not specifically bind to either promoter regions or a clear DNA consensus sequence (7). In streptomycetes and *C. glutamicum*, WhiA requires for its activity the auxiliary transcription factor WhiB (called WhcD in *Corynebacterium*) (5, 18, 19). However, homologues of these proteins are not present in *B. subtilis*. The WhiA protein is also not required for sporulation in *B. subtilis*, and it is still unclear what function WhiA fulfils in this model organism. We noticed that the space between nucleoids in *whiA* mutants is slightly larger than in wild-type cells, which prompted us to investigate whether WhiA is important for chromosome segregation. Interestingly, it appeared that the removal of either the chromosome replication and segregation regulator ParB or the DNA replication inhibitor YabA is synthetic lethal in a *whiA* mutant background. Extensive genetic, cell biology, and transcription studies revealed that this phenotype could be attributed to the induction of the SOS response and cell division inhibitor YneA. However, this DNA damage response appeared to be unrelated to the chromosome segregation defect observed in *whiA* mutant cells.

RESULTS

Nucleoid spacing. When nucleoids of exponentially growing Δ*whiA* cells were observed under the microscope, they seemed to be further segregated than those of wild-type cells (Fig. 1). Figure 1 shows data from cells grown in rich (LB) medium, and the *whiA* mutant grows slower in this medium than do wild-type cells (Fig. 1A). In Spizizen minimal salt medium (SMM), there is no clear growth rate difference between *whiA* mutant and wild-type cells (see Fig. S1 in the supplemental material). However, also in SMM, the nucleoids of the Δ*whiA* mutant cells are localized further apart (Fig. S1), indicating that this increased nucleoid spacing was not due to growth rate differences. The Δ*whiA* mutant that we used was a markerless mutation, containing a stop codon at the beginning of the gene (32 bp from start codon), ruling out any polar effect on downstream genes.

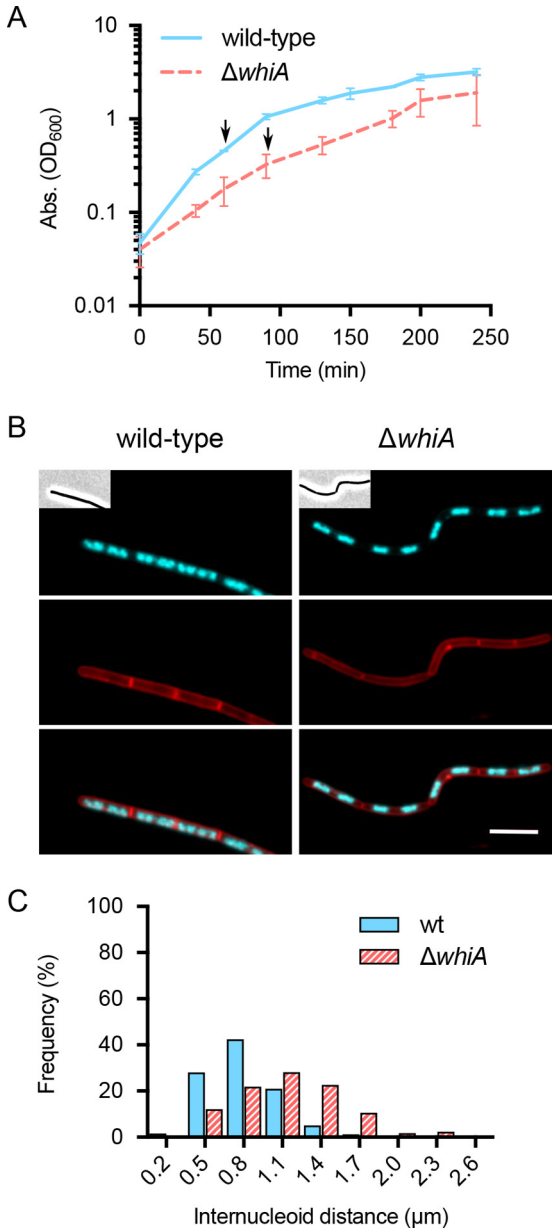

FIG 1 Increased internucleoid distances. (A) Growth curve of wild-type and Δ*whiA* cells (strain KS696) grown in LB medium at 37°C. (B) Wild-type and Δ*whiA* cells from the culture in A (arrows) were stained with DAPI (cyan) and FM-95 (red) dye to mark nucleoids and cell membranes, respectively. Scale bar is 5 μm. (C) Internucleoid distances in wild-type (wt) and Δ*whiA* mutant cells (n = 649 and 512, respectively). Two biological independent replicates were performed, yielding similar results (not shown).

The increase in nucleoid spacing suggested that WhiA could affect chromosome replication or segregation. To examine this, we looked at the localization of green fluorescent protein (GFP)-tagged proteins, including ParB involved in chromosome replication and segregation (20–22), the bacterial condensin homolog SMC (Structural Maintenance of Chromosomes) involved in chromosome condensation and segregation (23, 24), the DNA polymerase beta subunit DnaN (25, 26), the replication terminator protein Rtp (27, 28), and the DNA packaging protein Hbsu (29, 30). These proteins show distinct DNA localization patterns related to their activities (Fig. 2). ParB and SMC accumulate around and close to the origins of replication (24, 31). The DNA replisome, marked by DnaN-GFP, forms foci at the center of nucleoids (32, 33). Rtp binds to chromosome termini, and Hbsu covers the complete nucleoid (29). However, as indi-

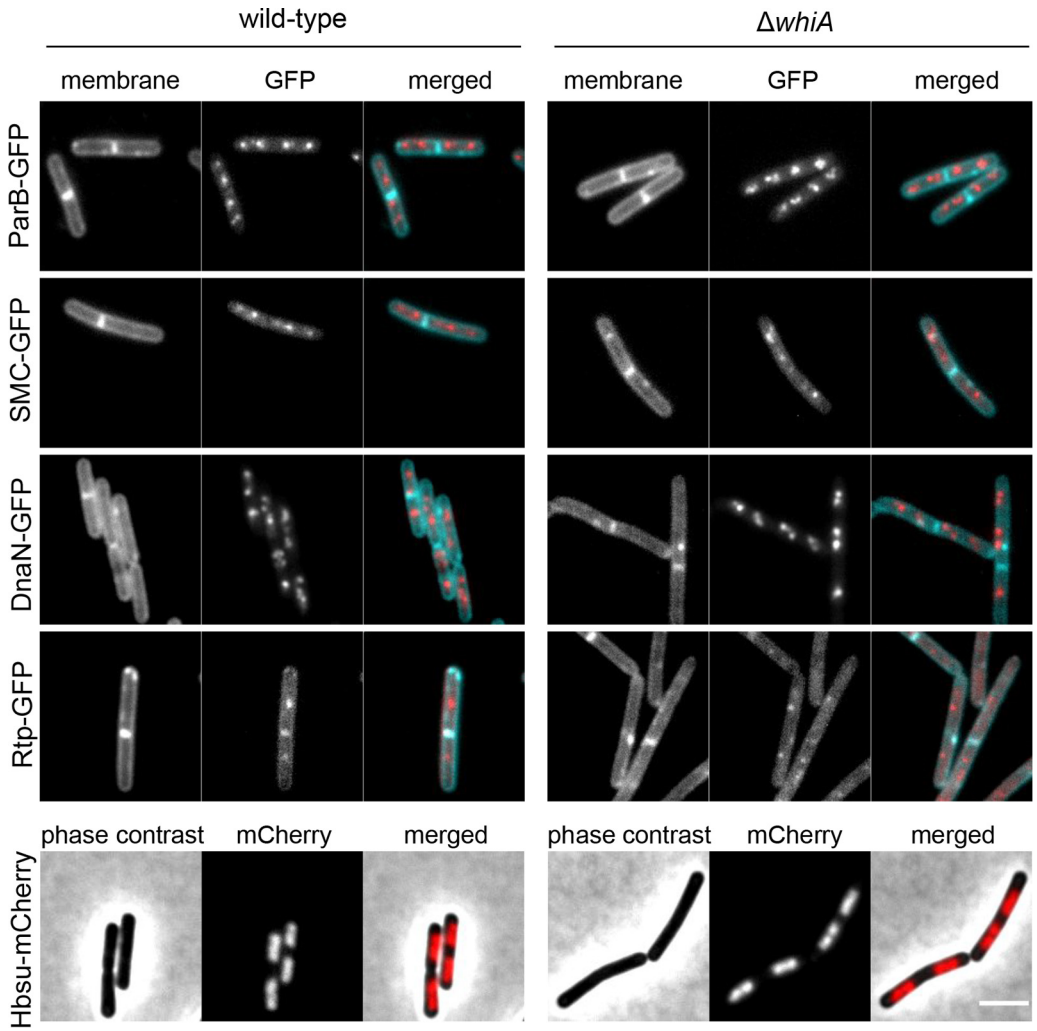

FIG 2 Lack of WhiA does not alter the localization of proteins involved in DNA replication and segregation. Fluorescence microscopy of exponentially growing wild-type and Δ*whiA* mutant cells containing different GFP-reporter constructs related to DNA replication and segregation. ParB, SMC, DnaN, and Rtp were fused to GFP, and Hbsu was fused to mCherry. See the text for details. Cell membranes were stained with FM-95. Scale bar is 3 μm. Examples of more cells are shown in Fig. S2.

cated in Fig. 2, we did not notice any difference in the cellular localization of these proteins between wild-type and Δ*whiA* mutant cells. The number of ParB foci was also unaffected (Fig. S3A). To check whether chromosomes were more condensed in the *whiA* mutant, the lengths and widths of Hbsu-mCherry labeled nucleoids were measured. Again, we did not notice significant differences between wild-type and Δ*whiA* mutant cells (Fig. S3B and C).

WhiA becomes essential when ParAB are absent. The DNA replication initiator protein DnaA binds to the origin of replication gene (*oriC*) and recruits the DNA replisome (34–36). ParA activates DnaA, whereas ParB inhibits the activity of ParA (31, 37, 38). ParB also has a role in DNA compaction and segregation, since it promotes the recruitment of the SMC complex to *oriC* (23, 24). Normally, the absence of ParA and ParB does not result in a noticeable growth defect. However, when we tried to introduce a Δ*whiA* mutation into a Δ*parAB* background, only a few transformants were obtained that grew slowly (Fig. 3A), and it was not possible to grow them up in liquid medium.

To confirm that the absence of WhiA in the Δ*parAB* background was lethal, we placed *whiA* under the control of the isopropyl-β-D-thiogalactopyranoside (IPTG)-

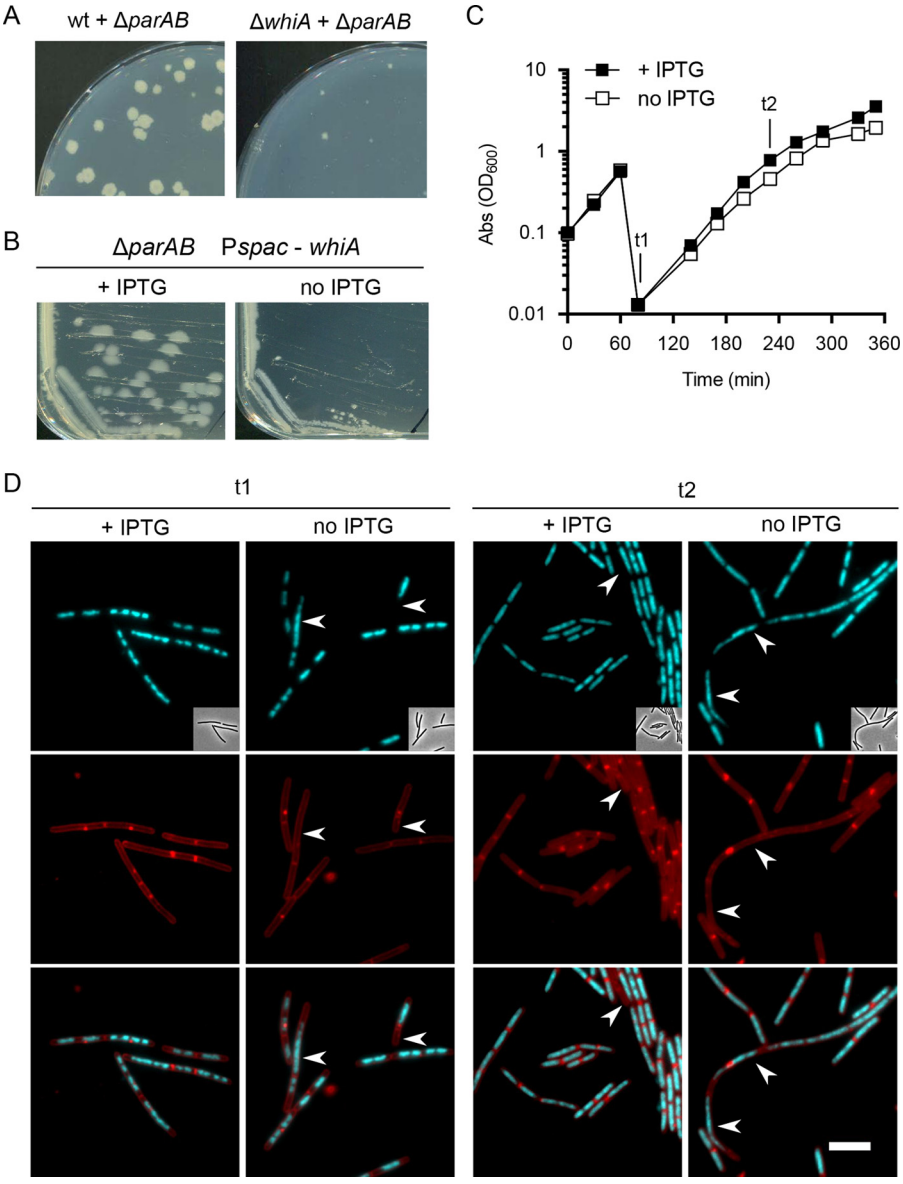

FIG 3 WhiA is essential in a Δ*parAB* mutant. (A) Transformants of either wild-type (wt) cells or Δ*whiA* cells transformed with Δ*parAB* genomic DNA. (B) Strain LB53, containing the Δ*parAB* mutation and an IPTG-inducible *whiA* allele, streaked out on plates with and without 0.1 mM IPTG. (C) Growth curves of strain LB53 grown in LB in the presence or absence of 0.1 mM IPTG. After 60 min, the culture was diluted into fresh medium. (D) At t1 and t2, samples were taken for microscopic analyses: fluorescence microscopy images of cells stained with DAPI (cyan) and FM-95 dye (red) to mark nucleoids and membranes, respectively. Scale bar is 5 μm. Arrowheads indicate anucleate cells and cells with aberrant nucleoids. Examples of more cells are shown in Fig. S4.

inducible P*spac* promoter, by means of a Campbell integration (see Materials and Methods for details). An extra copy of *lacI* was introduced at the ectopic *aprE* locus to increase the LacI concentration, ensuring a tight regulation of the P*spac* promoter. As shown in Fig. 3B, the resulting strain (strain LB53) was unable to form normal colonies when IPTG was absent. In liquid medium, the effect of WhiA depletion took several generations before it became noticeable and the optical density (OD) leveled off (Fig. 3C). However, microscopic examination revealed that after approximately 1.5 h of growth without IPTG, the number of cells with aberrant nucleoids became apparent, and after two more hours, the percentages of anucleate cells and cells with nonsegregated nucleoids had risen from 0.1% to 0.6% and 1.7% to 4.3%, respectively, while the

number of cells with dissected nucleoids increased from 0% to 2.5% (~750 cells counted) (Fig. 3D, t2, and S4).

DNA replication initiation. The *parAB* genes form a bicistronic operon. To determine whether the synthetic lethal phenotype was caused by the absence of ParB alone, the IPTG-inducible *whiA* allele was introduced in a wild-type, Δ*parA* mutant, and Δ*parB* mutant background strain (resulting in strains LB36, LB418, and LB419, respectively). The Δ*parA* mutant was constructed so that expression of Δ*parB* was unaffected (31). A spot dilution assay was used to assess viability when grown in the absence of IPTG. As shown in Fig. 4A, depletion of WhiA in the Δ*parB* background has the same detrimental effect on colony formation as WhiA depletion in the Δ*parAB* background, whereas there was no effect in the wild-type background, and the effect on the Δ*parA* background was only mild.

Since the absence of ParB results in the stimulation of ParA and overinitiation of DNA replication (31), it might be that this effect is lethal when WhiA is absent. To corroborate this, we tested a *yabA* mutant. YabA is a direct inhibitor of DnaA, and the absence of *yabA* also results in overreplication (39). We combined the Δ*yabA* knockout with the IPTG-inducible *whiA* allele (strain LB534), and as shown in Fig. 4A, depletion of WhiA in the Δ*yabA* background severely affected growth as well.

These data might suggest that replication initiation is affected in a Δ*whiA* mutant. To test this, we analyzed the origin copy number by determining the origin-to-terminus ratio (ori/ter ratio) using quantitative PCR (qPCR) (31). Two *whiA* mutants were tested, strain KS400 containing a kanamycin resistance cassette insertion, and the markerless *whiA* mutant (strain KS696). As controls, wild-type cells and Δ*parB* mutant cells (strain KS382) were used. The different strains were grown in LB medium at 37°C until mid-log phase, after which the ori/ter ratio was determined. Surprisingly, the ori/ter ratio appeared to be unaffected in the *whiA* mutants (Fig. 4B), indicating that the synthetic lethal phenotype is not directly related to DNA replication initiation.

Suppressor mutations. As described in the introduction, the Δ*whiA* mutation is synthetic lethal when *zapA* is knocked out, and this phenotype can be suppressed by inactivation of the glucosyltransferase UgtP (7). To determine whether this phenotype is different from the synthetic lethal phenotype of the Δ*whiA* Δ*parAB* double mutant, we examined whether the deletion of *ugtP* could suppress the lethal Δ*whiA* Δ*parAB* combination. To this end, the IPTG-inducible *whiA* allele was introduced into a Δ*parAB* Δ*ugtP* double-mutant background, which also contained an extra copy of *lacI* to allow tighter regulation of the P*spac* promoter (strain LB630). However, a spot dilution assay of this strain grown in the presence and absence of IPTG showed that the Δ*ugtP* mutation did not restore viability when WhiA was depleted (Fig. 4C). This was also not the case when PgcA, which provides the UDP-glucose substrate for the glucosyltransferase UgtP, was absent (Fig. 4C), whereas such a mutation restores the growth of the Δ*whiA* Δ*zapA* double mutant (7). A deletion of *pgcA* was also not able to restore viability when WhiA was depleted in the Δ*yabA* background (strain LB728) (Fig. 4C). These results indicated that the synthetic lethality of both the Δ*whiA* Δ*parAB* and the Δ*whiA* Δ*yabA* double mutants is related to a different pathway from the one that is affected in the Δ*whiA* Δ*zapA* double mutant.

Transcriptome analysis. To better understand what causes lethality when both *whiA* and *parAB* are absent, we analyzed the effect on the transcriptome using RNA sequencing (RNA-seq). Strain LB53 containing the conditional P*spac-whiA* allele, an extra copy of *lacI*, and the Δ*parAB* mutation (see Fig. 3) was grown in LB with 0.1 mM IPTG, washed, and resuspended in prewarmed LB medium with or without 0.1 mM IPTG. After approximately 100 min of growth (OD at 600 nm [OD_{600}], ~0.5), cells were harvested for RNA isolation. This time period was chosen since aberrant nucleoids became visible in the culture without IPTG, yet the growth rate was still normal, reducing secondary effects due to growth retardation.

The volcano plot in Fig. 5 shows the fold change relative to the *P* values. The expression differences (fold change) appeared to be surprisingly limited considering

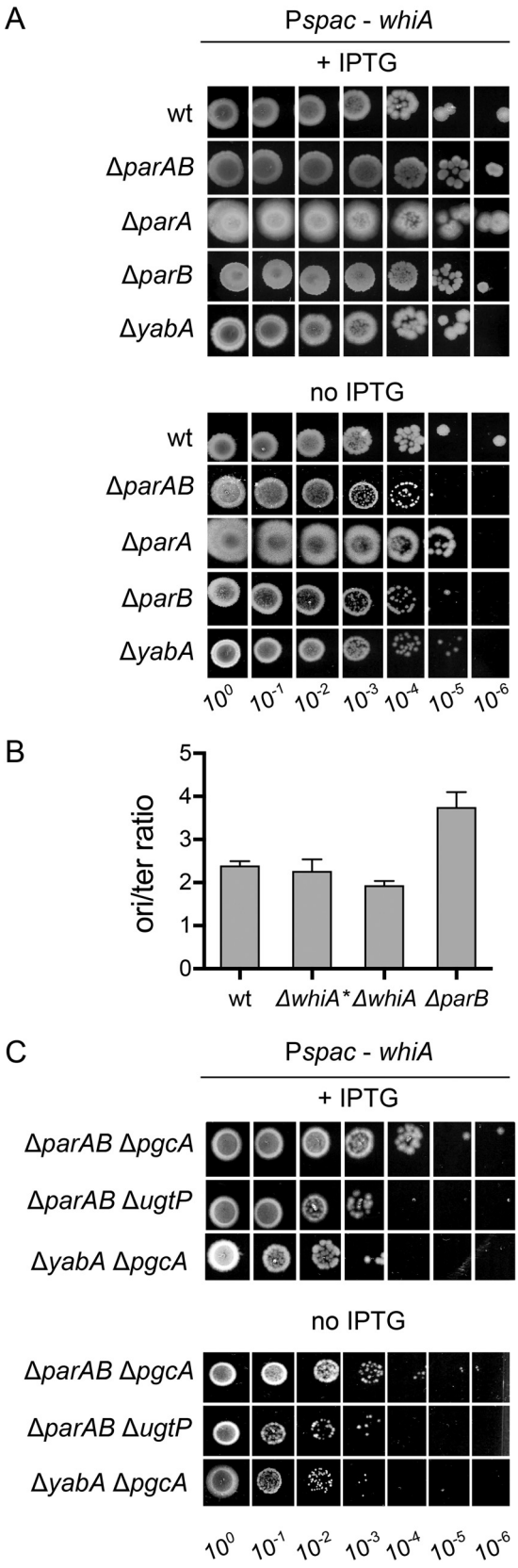

FIG 4 WhiA depletion effects on colony formation and DNA replication initiation. (A) Viability of WhiA depletion in either a wild-type (strain LB36), Δ*parAB* mutant (strain LB53), Δ*parA* mutant (strain LB418), Δ*parB* mutant (strain LB419), or Δ*yabA* mutant (strain LB534) genetic background assessed using a spot

(Continued on next page)

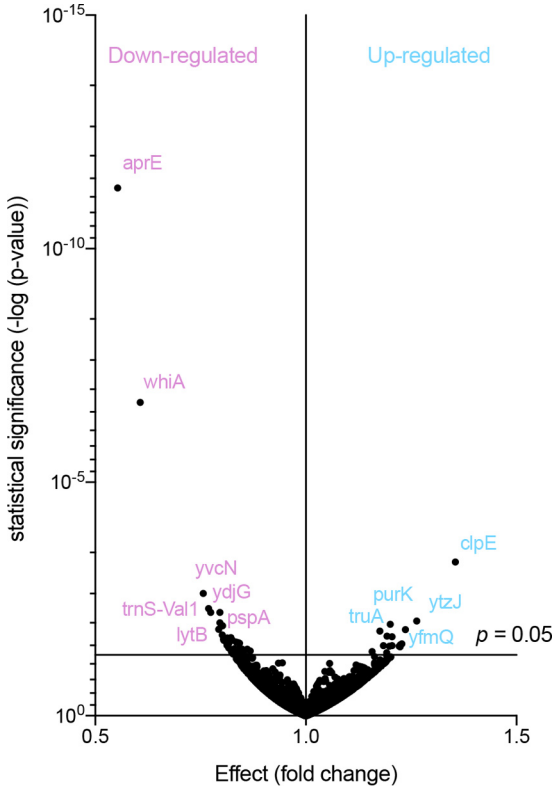

FIG 5 Transcriptome analysis. Volcano plot depicting the transcriptome data as a relation between *P* value and fold change. See main text for details. RNA levels of LB53 cells grown in the presence of IPTG were divided by those of cells grown in the absence of IPTG (WhiA depletion condition). Main downregulated and upregulated genes in the WhiA-depleted cells are shown. See also Table 1, which lists 23 differentially expressed genes.

the clear phenotypic difference, and their downregulation varied between 1.4-fold upregulated and 0.6-fold. Table 1 lists 23 differentially expressed genes with an adjusted *P* value of <0.05 and fold difference of >0.5. The downregulation of *whiA* was apparent, although the fold change of only 0.6 suggested that there was still a substantial amount of *whiA* mRNA left in cells grown without IPTG. The downregulation of *aprE* was an artifact caused by the extra *lacI* gene inserted into the *aprE* locus. *yvcN* is located downstream of *whiA* in the operon and therefore is downregulated in cells grown without IPTG. The most upregulated (1.4-fold) gene was *clpE*, encoding a chaperone normally upregulated during heat shock (40). Another upregulated stress gene was the essential chaperone *groEL* (1.2-fold). In a previous transcriptome study of a *whiA* mutant, *clpE* was also upregulated (7). In the list of downregulated genes, we found only one stress gene, *pspA* (0.8-fold), involved in membrane stress (41). In conclusion, a reduction in WhiA seems to affect protein folding, but the transcriptome data did not provide a clear explanation as to why the absence of WhiA is lethal in the Δ*parAB* background.

SOS response. The RNA-seq data did not show induction of DNA repair (SOS) genes. This was remarkable considering the observed nucleoid segregation. To ensure that the

FIG 4 Legend (Continued)
dilution assay. *whiA* was expressed from an IPTG-inducible promoter (P*spac*). Exponential growing cells (with IPTG) were diluted and spotted onto agar plates with (0.1 mM) or without IPTG. (B) ori/ter ratio of wild-type markerless *whiA* mutant (Δ*whiA**, strain KS696), Δ*whiA* mutant (strain KS400), and Δ*parB* mutant (strain HM42) cells growing exponentially in LB at 37°C (two biological replicates). (C) Viability of WhiA depletion in either a Δ*parAB* Δ*pgcA* (strain LB629), Δ*parAB* Δ*ugtP* (strain LB630), or Δ*yabA* Δ*pgcA* (strain LB728) genetic background assessed using a spot dilution assay. Growth conditions were the same as those described for panel A.

TABLE 1 Transcriptome analysis of strain LB53 grown in the absence or presence of IPTG[a]

Gene	FC	*P* value	Function
Upregulated			
clpE	1.4	0.0005	ATPase subunit of the ClpE-ClpP protease
purK	1.2	0.0110	Purine biosynthesis
purE	1.2	0.0199	Purine biosynthesis
ytzJ	1.3	0.0094	Unknown protein
yfmQ	1.2	0.0143	Unknown protein
truA	1.2	0.0153	tRNA modification, pseudouridylate synthase I
yabE	1.2	0.0202	Similar to cell wall binding protein
yobE	1.2	0.0287	Similar to general secretion pathway protein
ywdA	1.2	0.0302	Unknown protein
guaC	1.2	0.0315	Purine salvage and interconversion, GMP reductase
groEL	1.2	0.0317	Protein folding and refolding, chaperonin
Downregulated			
aprE	0.5	5.02E−12	Countertranscript from integrated *lacI* copy
whiA	0.6	1.95E−7	
yvcN	0.8	0.0024	*whiA* operon, unknown protein
pspA	0.8	0.0141	*pspA* operon, cell envelope stress proteins
ydjG	0.8	0.0050	*pspA* operon, unknown protein
ydjH	0.8	0.0118	*pspA* operon, unknown protein
ydjI	0.8	0.0061	*pspA* operon, unknown protein
lytB	0.8	0.0103	Modifier protein of major autolysin LytC
trnSL-Val1	0.8	0.0061	Translation, tRNA-Val
trnB-Arg	0.8	0.0214	Translation, tRNA-Arg
trnJ-Val	0.8	0.0225	Translation, tRNA-Val
yhfS	0.8	0.0214	Similar to acetyl-CoA C-acetyltransferase[b]
yopJ	0.8	0.0187	Unknown protein

[a]LB53 contains the Δ*parAB* mutation and *whiA* under the control of the IPTG-inducible P*spac* promoter. An extra *lacI* repressor was inserted into the *aprE* locus. Genes with a *P* value of <0.05 and fold change (FC) of >0.5 are listed. The data are based on three biological replicates.
[b]CoA, coenzyme A.

key SOS protein RecA was not activated, we looked at the localization of a GFP-RecA reporter fusion (strain LB583). Normally, RecA localizes throughout the cell and is enriched at nucleoids; however, after DNA damage, RecA is activated and forms large filaments over the nucleoid (42) (Fig. 6A). These RecA nucleofilaments mediate homologous DNA pairing (43). After depleting WhiA in the Δ*parAB* knockout by growing cells without IPTG for approximately an hour, GFP-RecA filaments became visible (Fig. 6B). These filaments were not observed when cells were grown with IPTG (Fig. 6B) and were also not observed in the Δ*whiA* single mutant (Fig. 6A). The same results were obtained when WhiA was depleted in the Δ*yabA* background (Fig. S5).

These data suggested that WhiA is somehow important for DNA integrity. If that is the case, it is likely that a Δ*whiA* mutant is more sensitive to DNA-damaging agents. To test this, the Δ*whiA* mutant strain containing the kanamycin resistance cassette and the clean *whiA*-knockout strain (Δ*whiA** mutant) were exposed on a plate to the DNA-damaging agent mitomycin C in a colony spot assay. As shown in Fig. 7A, both *whiA* mutants were highly sensitive to mitomycin C. In fact, we were unable to obtain a Δ*whiA* Δ*recA* double knockout (data not shown). Figure 7A also shows that the Δ*parAB* mutant itself was not that much more sensitive to mitomycin C than wild-type cells.

Cell division inhibitor YneA. In many bacteria, the SOS response blocks cell division, and in *B. subtilis*, YneA is responsible for this blockage (44). The protein inhibits FtsZ polymerization by an as-yet-unknown mechanism (45). Since previous research showed that WhiA is required for cell division under certain conditions, the question arises as to whether the activation of YneA due to DNA damage and subsequent SOS response cause the sensitivity of the Δ*whiA* mutant for mitomycin C. To test this, we removed the *yneA* operon (Δ*yneABC*) in the Δ*whiA* mutant. Indeed, as shown in Fig. 7A, the removal of YneA increases the resistance of the Δ*whiA* mutant to mitomycin C.

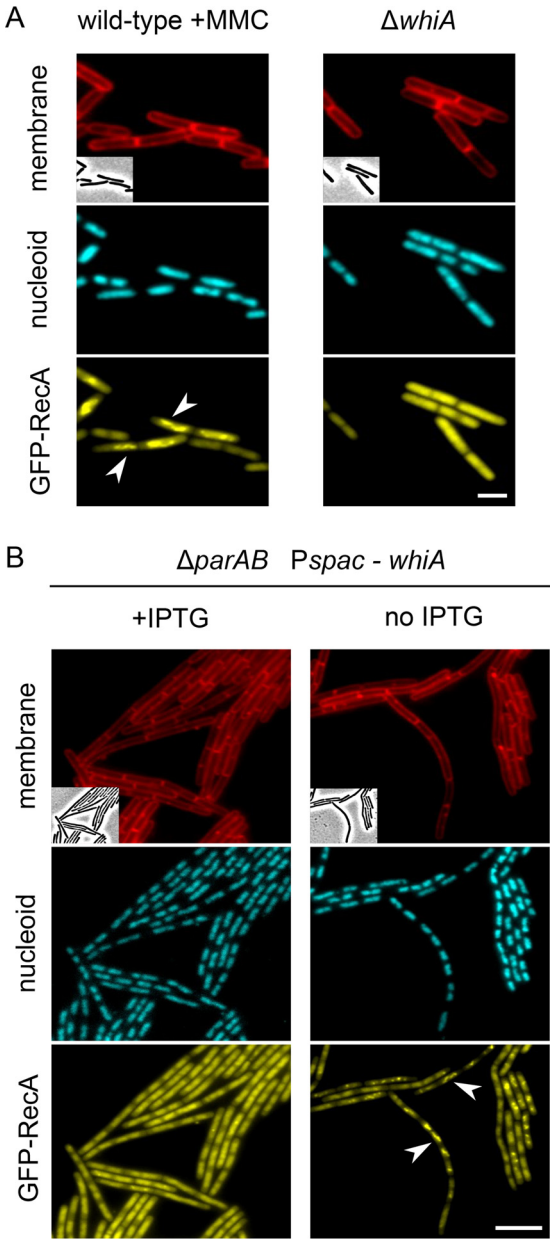

FIG 6 Depletion of WhiA in a Δ*parAB* mutant activates RecA. (A) Left, fluorescence microscopy images of exponentially growing wild-type cells expressing a GFP-RecA reporter (strain UG10) exposed to a sublethal concentration (50 ng/ml) of mitomycin C for 1 h (+MMC). Right, Δ*whiA* mutant cells expressing a GFP-RecA reporter (strain LB557). (B) Fluorescence microscopy images of Δ*parAB* mutant strain LB583 expressing the GFP-RecA reporter and *whiA* under the control of the IPTG-inducible P*spac* promoter. Cells were grown in the presence or absence of IPTG for 1 h. Cells were stained with DAPI (cyan) and FM-95 (red) to mark nucleoids and cell membranes, respectively. Arrowheads indicate RecA filaments. Scale bars for panels A and B are 2 μm and 5 μm, respectively.

Importantly, when the Δ*yneABC* mutation was introduced in the Δ*parAB* background, it became possible to deplete WhiA without greatly affecting colony formation (Fig. 7B). In fact, we were able to obtain a Δ*yneABC* Δ*parAB* Δ*whiA* triple knockout (Fig. S6 and S7). However, this triple mutant still showed a high frequency of aberrant nucleoids, similar to what was observed when WhiA was depleted in the Δ*parAB* background (Fig. 7C and S4B). Nevertheless, cell length was restored and comparable to that of wild-type cells (Fig. S6C). Clearly, the lethality of the Δ*whiA* Δ*parAB* double mutant is caused by a blockage of cell division.

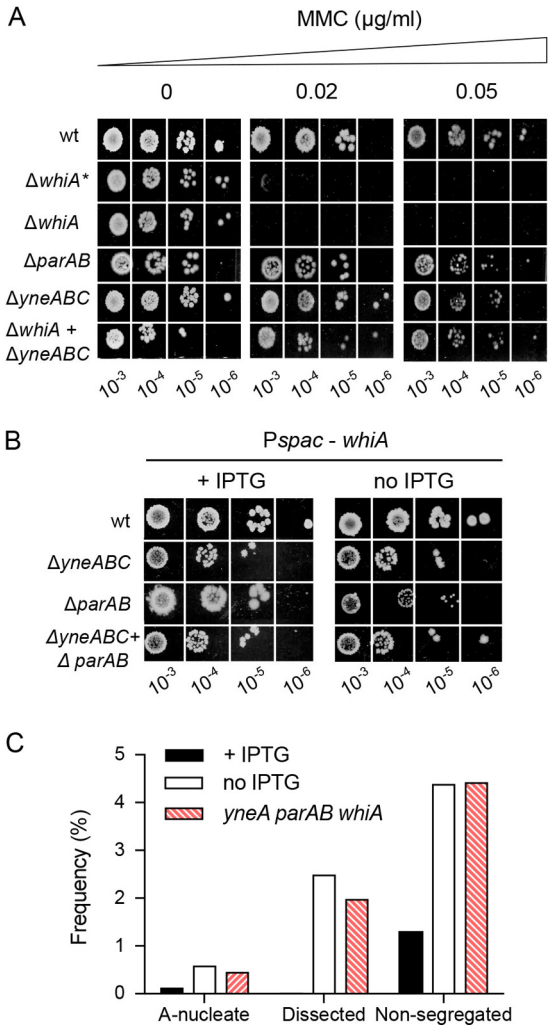

FIG 7 Δ*whiA* mutant sensitive to DNA damage is repressed by Δ*yneABC* mutation. (A) Viability of cells exposed to increasing concentrations of mitomycin C (MMC). The following strains were used: wt (strain 168), Δ*whiA** mutant (markerless *whiA* point mutant, strain KS696), Δ*whiA* mutant (strain KS400), Δ*parAB* mutant (strain HM1), Δ*yneABC* mutant (strain YK138), and Δ*yneABC* Δ*whiA* mutant (strain LB438). (B) Viability was restored when YneA was absent. The strains contained the IPTG-inducible *whiA* allele and an extra *lacI* copy (strain LB36), including either the Δ*yneABC* (strain LB516), Δ*parAB* (strain LB53) or Δ*yneABC* Δ*parAB* mutation (strain LB525). (C) Quantification of aberrant nucleoids grouped by anucleate cells, cells with dissected chromosomes, and cells with nonsegregated chromosomes. Strain LB53 was grown in the presence or absence of IPTG for 2.5 h (time point t2 in Fig. 3). Strain LB460 containing the Δ*yneABC* Δ*parAB* Δ*whiA* triple mutation was grown to mid-exponential phase (+IPTG, $n = 763$; no IPTG, $n = 843$; and LB460, $n = 655$).

SOS induction. The above-mentioned results suggested that the induction of YneA was the primary cause for the observed synthetic lethal phenotype. However, there was no evidence for SOS induction in our transcriptome data. Possibly, the relatively short depletion time of 100 min, which reduced *whiA* levels by only 0.6-fold, was not sufficient to activate the SOS response. To check this, we measured *yneA* and *recA* expression by constructing β-galactosidase (*lacZ*) promoter reporter fusions. The promoter fusions were inserted into the Δ*parAB* P*spac-whiA* strain, resulting in strains LB649 and LB648, respectively. Compared to wild-type cells, there is a clear induction of both the *yneA* and *recA* promoters (Fig. 8B and D, compare left and middle columns). However, there was no difference between growth in the presence and absence of IPTG. This suggested that the SOS response was already activated by the absence of ParAB alone. Indeed, when we transformed the promoter reporters into the Δ*parAB* and Δ*whiA* single-mutant strains, we

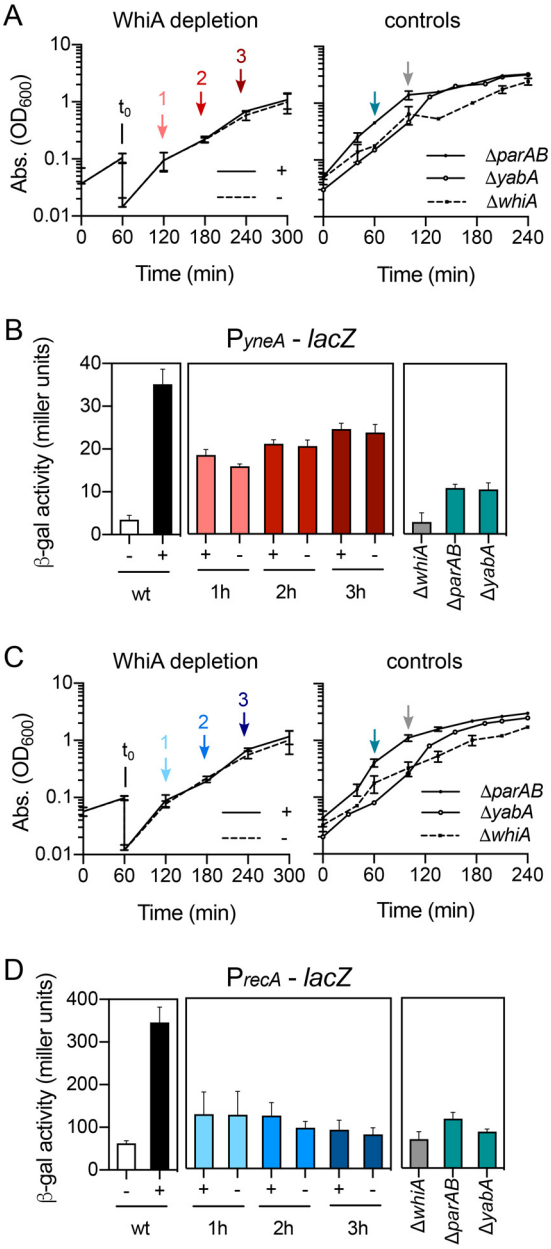

FIG 8 *yneA* and *recA* are activated in Δ*parAB* and Δ*yabA* mutants. Promoter activities of *yneA* and *recA* were measured using the β-galactosidase-expressing *lacZ* reporter. (A and C) Cells were grown in LB at 37°C, and samples were taken at the indicated time points (arrows). (B and D) *lacZ* expression. Left images, induction after mitomycin C (50 ng/ml) exposure (+) of wild-type cells for 1 h. Middle images, *lacZ* expression after 1 h, 2 h, and 3 h of growth with 0.1 mM IPTG (+) or without IPTG (−) to deplete WhiA in a Δ*parAB* background. Right images, *lacZ* expression in the single Δ*whiA*, Δ*parAB*, and Δ*yabA* backgrounds. Strains used were LB642 (P*yneA-lacZ*), LB641 (P*recA-lacZ*), LB649 (P*yneA-lacZ* Δ*parAB* P*spac-whiA aprE-lacI*), LB648 (P*recA-lacZ* Δ*parAB* P*spac-whiA aprE-lacI*), LB654 (P*yneA-lacZ* Δ*whiA*), LB652 (P*recA-lacZ* Δ*whiA*), LB655 (P*yneA-lacZ* Δ*parAB*), and LB653 (P*recA-lacZ* Δ*parAB*), LB720 (P*recA-lacZ* Δ*yabA*), and LB722 (P*yneA-lacZ* Δ*yabA*).

observed a clear activation of both promoters in the Δ*parAB* background but not in the Δ*whiA* background (Fig. 8B and D, right columns). In fact, these promoters were also more active in a Δ*yabA* background (Fig. 8B and D, right panels). Thus, the synthetic lethality of WhiA depletion in Δ*parAB* and Δ*yabA* mutant strains is caused by the constitutive expression of YneA in these backgrounds. This also explains why we did not observe SOS induction in the transcriptome experiment, as both the IPTG-grown and non-IPTG-grown samples contained the Δ*parAB* mutation.

DISCUSSION

Despite the fact that WhiA is conserved in Gram-positive bacteria and is required for optimal growth in *B. subtilis*, surprisingly little is known about its mechanistic role. The only other organisms in which the function of WhiA has been studied are streptomycetes and *C. glutamicum*, and in these organisms, the protein functions as a transcription factor (4, 5, 19). In *B. subtilis*, WhiA also binds DNA, but the protein does not bind specifically to promoter regions and does not seem to function as a transcription factor in this organism (7).

Previously, we have shown that WhiA becomes essential in *B. subtilis* when either *zapA*, *minCD*, *ezrA*, or *noc* is deleted. MinCD and Noc inhibit the polymerization of FtsZ, and ZapA and EzrA bind to FtsZ to form the Z-ring. In the current study, we have shown that a Δ*whiA* mutation is very sensitive for the induction of the SOS response-related cell division inhibitor YneA, which delays FtsZ-ring assembly (45). This fits well with our previous findings that pointed toward a functional role of WhiA in the assembly of the Z-rings. However, we argue that the functional role of WhiA is more complicated and extends to chromosome maintenance.

First, we were unable to construct a Δ*whiA* Δ*recA* double knockout. RecA cleaves LexA, the transcriptional repressor of the SOS regulon (46), and RecA is necessary for the induction of *yneA* (44). Therefore, the synthetic lethality of a Δ*whiA* Δ*recA* double knockout suggests that WhiA is required for processes other than Z-ring formation. Second, a Δ*whiA* mutant shows an increased distance between nucleoids, indicative of a chromosome segregation defect, and this defect is not restored when *yneA* is deleted. Third, depletion of WhiA in the Δ*parAB* background not only caused cell filamentation, indicative of cell division blockage, but it also resulted in anucleate cells and cells with deformed nucleoids, which again are not restored when YneA is absent.

As far as we know, SOS induction in *parAB* mutants has not been reported before. ParB is involved in loading of the bacterial condensin homolog SMC onto the chromosome (23, 24), and the absence of ParB interferes with both segregation and organization of the genome (47, 48). SMC also interacts with the DNA helicase AddAB, which is essential for recombinational DNA repair, and an *smc* mutant is highly sensitive for mitomycin C (49). Possibly, the impaired loading of SMC onto the chromosome in the absence of ParB interferes with its interaction with AddAB and may therefore lead to activation of the SOS response in a *parAB* mutant. However, the deletion of *yabA* also induces the SOS response. YabA interacts with DnaA and prevents the proper oligomerization of DnaA on *oriC* (50). YabA also tethers DnaA to the polymerase clamp protein DnaN (51). Possibly, the activation of the SOS response in the Δ*yabA* mutant is related to this, since DnaN serves as a platform for mismatch detection and coupling of repair to DNA replication (52). On the other hand, the absence of both ParB and YabA leads to overreplication of DNA, and it is plausible that this will cause problems when DNA segregation is affected, as is the case in cells lacking WhiA.

In conclusion, in *B. subtilis* WhiA seems to play a role in both cell division and DNA segregation. This pleiotropic role suggests that the protein is involved in a rather basal cellular process, which explains why WhiA is conserved and is even present in the reduced genomes of mycoplasmas.

MATERIALS AND METHODS

Bacterial strains and growth conditions. Luria-Bertani (LB) medium was used for routine selection and maintenance of both *B. subtilis* and *Escherichia coli* strains. Minimal medium was based on Spizizen's minimal medium (SMM) (53) and consisted of 2 g/liter $(NH_4)_2SO_4$, 14 g/liter K_2HPO_4, 6 g/liter KH_2PO_4, 1 g/liter sodium citrate, 2 g/liter $MgSO_4$, 5 g/liter glucose, 2 g/liter tryptophan, 0.2 g/liter Casamino Acids, and 2.2 g/liter ammonium ferric citrate. All strains were grown at 37°C, or at 30°C when GFP reporter fusions were expressed. Supplements were added at the following concentrations: 20 mg/ml tryptophan, 100 mg/ml ampicillin, 5 mg/ml chloramphenicol, 5 mg/ml kanamycin, 100 mg/ml spectinomycin, 10 mg/ml tetracycline, 1 mg/ml erythromycin, 0.1 mM IPTG, and 0.1% (wt/vol) xylose. The *B. subtilis* strains used in this study are listed in Table S1 in the supplemental material. The mutant strains provided by other labs were transformed into our laboratory strain to ensure isogenic backgrounds.

WhiA depletion strains were always grown in the presence of the selection marker (erythromycin), due to the Campbell type integration of the P*spac-whiA* construct into the *whiA* locus. Cells from a single colony were inoculated into LB medium with 0.1 mM IPTG and grown at 37°C to an OD_{600} of ~1. Subsequently, the cells were harvested, washed in prewarmed LB medium, resuspended to an OD_{600} of 0.01, and grown in the absence of IPTG.

Strain constructions. Molecular cloning, PCRs, and transformations were carried out by standard techniques. The plasmids and oligonucleotides used in this study are listed in Tables S2 and S3, respectively.

The *whiA* gene was deleted by replacing its coding sequence with a *tet* resistance cassette. The region approximately 4 kb upstream and downstream of the coding sequence of *whiA* was amplified using the LH10-LH11 and LH12-LH13 oligonucleotide pairs, and using the genomic DNA of strain 168 as the template. The *tet* cassette was amplified using the oligonucleotides LH7-LH8 and the plasmid pBEST309 (54) as the template. BamHI and PstI restriction sites were inserted into the primers. The PCR fragments were digested with the same restriction enzymes, and the ligation reaction mixture was assembled with equimolar concentrations of each fragment in a total volume of 10 μl. Competent cells of *B. subtilis* were directly transformed with the ligation reaction. Transformants were selected on antibiotic plates and verified by PCR, restriction enzyme digestion, and sequencing, and the resulting strain was labeled LB21.

Plasmid pMutiYvcL (7) was transformed into *B. subtilis*, resulting in single-crossover (Campbell type) integration positioning the IPTG-inducible P*spac* promoter upstream of *whiA*. To allow tight regulation of *whiA* expression, an extra copy of *lacI* was introduced by transforming plasmid pAPNC213 (55), which integrates into the *aprE* locus and contains a *lacI* gene, resulting in strain LB36. Competent cells of the strain LB36 were transformed with genomic DNA of a Δ*parAB* mutant (strain HM31) (31), resulting in strain LB53.

A xylose-inducible GFP-RecA fusion was constructed as follows. A PCR fragment containing *recA* was amplified with the UG01b-UG02b oligonucleotide pair and genomic DNA of strain 168 as the template. XhoI and EcoRI restriction sites, a flexible linker, and terminator were inserted into the primers. The PCR product and the *amyE* integration vector pSG1729 (56) were digested with XhoI and EcoRI restriction enzymes and ligated. The resulting plasmid was verified by sequencing and transformed into *B. subtilis* competent cells, resulting in strain UG10.

recA and *yneA* promoter reporters were constructed by amplifying the promoter regions with the LB141-LB142 and LB145-LB146 primer pairs, respectively, and using the genomic DNA of strain 168 as the template. The *amyE* integration vector pPG40 (57) containing the β-galactosidase gene (*lacZ*) was amplified with the LB139-LB140 and LB143-LB144 primer pairs for cloning PrecA and PyneA, respectively. Overlapping sequences (20 nucleotides [nt]) were inserted into the primers to the adjacent sequences of interest for cloning using the one-step isothermal assembly method (58). In short, equimolar concentrations of the two DNA fragments sharing terminal sequence overlaps (20 nt) were mixed with T5 exonuclease (New England BioLabs [NEB]), Phusion high-fidelity DNA polymerase (NEB), and *Taq* DNA ligase (NEB) in a total volume of 10 μl. The reaction mixtures were incubated at 50°C for 1 h. The resulting plasmids pLB74 and pLB75 were verified by restriction enzyme digestion and sequencing and transformed into *B. subtilis* competent cells, resulting in strains LB641 and LB642, respectively.

The *parA* single mutant (strain HM161) was constructed elsewhere (31) and was transformed into our laboratory wild-type strain to ensure an isogenic background (strain KS383). The *parA* in-frame deletion was designed so that expression of ParB is not affected (Heath Murray, personal communication).

Microscopy. Membranes were stained with the fluorescent dye FM-95, and the DNA was stained with 4′,6-diamidino-2-phenylindole (DAPI). Cells were mounted on microscope slides covered with a thin film of 1% agarose. Microscopy was performed on an inverted fluorescence Nikon Eclipse Ti microscope. The digital images were acquired and analyzed with ImageJ version 1.48d5 (National Institutes of Health).

Quantitative PCR. To assess the ori/ter ratio, DNA isolation and qPCR were performed as previously described (31). In brief, cells were grown to exponential phase, and 0.5% sodium azide was added to 1 ml of cell suspension. The DNA was isolated using the DNeasy blood and tissue kit (Qiagen). For each PCR, 2 μl of the qORI-F-qORI-R or qTER-F-qTER-R primer pair (3 μM), 10 μl of SYBR green PCR master mix (Applied Biosystems), and 8 μl of 400×-diluted chromosomal DNA were mixed. The qPCR was performed using the Roche LightCycler 480 instrument. Spore DNA, where the ori/ter ratio is expected to be 1, was used to normalize the qPCRs. The relative ori/ter ratio was calculated from the difference in the cycle number when fluorescence crosses an arbitrary line ([Cp]).

Transcriptome analysis. Cells (2-ml cultures) were spun down (Eppendorf centrifuge at 14,000 rpm and 4°C for 30 s), resuspended in 0.4 ml ice-cold growth medium, and added to a screw-cap Eppendorf tube containing 1.5-g glass beads (0.1 mm), 500 μl phenol-chloroform-isoamyl alcohol (25:24:1), 50 μl 10% SDS, and 50 μl RNase-free water (59). All solutions were prepared with diethylpyrocarbonate (DEPC)-treated water. After vortexing, tubes were frozen in liquid nitrogen and stored at −80°C. Cells were broken using a bead beater for 4 min at room temperature. After 5 min of Eppendorf centrifugation (2 min, 10,000 rpm, 4°C), the water phase (~400 μl) was transferred to a clean tube containing 400 μl chloroform. After vortexing and centrifugation (2 min, Eppendorf centrifuge, 14,000 rpm, 4°C), the water phase (±300 μl) was transferred to a clean tube, and RNA was isolated with a High Pure RNA isolation kit (Roche Diagnostics GmbH, Mannheim, Germany). RNA was eluted in 50 μl elution buffer and quantified using a NanoDrop 1000 spectrophotometer (Thermo Scientific), yielding >3 μg total RNA per sample, a 260/230 ratio above 2.0, and a 260/280 ratio above 2.1. The TapeStation system (Agilent) was used for checking the integrity of the RNA, and RNA integrity number (RIN) values of 8.3 to 9.2 were obtained.

For next-generation sequencing, rRNA depletion was performed on the total RNA using the Ribo-Zero rRNA removal kit (Gram-positive bacteria) (Illumina). Barcoded RNA libraries were generated according to the manufacturer's protocols using the Ion Total RNA-seq kit version 2 and the Ion Xpress RNA-seq barcoding kit (Thermo Fisher Scientific). The size distribution and yield of the barcoded libraries were assessed using the 2200 TapeStation system with Agilent D1000 ScreenTape (Agilent Technologies). Sequencing templates were prepared on the Ion Chef system using the Ion PI Hi-Q Chef kit (Thermo Fisher Scientific). Sequencing was performed on an Ion Proton system using an Ion PI version 3 Chip (Thermo Fisher Scientific), according to the instructions of the manufacturer.

After quality control and trimming, the sequence reads were mapped onto the genome (genome build accession NCBI assembly no. GCA_000009045.1) using the Torrent Mapping Alignment Program (60). The Ion Proton system generates sequence reads of various lengths, and this program combines a short-read algorithm (61) and long-read algorithm (62, 63) in a multistage mapping approach. The gene expression levels were quantified using HTseq (64). The data were normalized and analyzed for differential expression using R statistical software and the DESeq2 package (65).

***β*-Galactosidase activity assay.** *β*-Galactosidase assays were performed as described by Daniel et al. (66) and enzymatic activity calculated as described by Miller (67).

SUPPLEMENTAL MATERIAL

Supplemental material for this article may be found at https://doi.org/10.1128/JB.00633-17.

SUPPLEMENTAL FILE 1, PDF file, 1.3 MB.

ACKNOWLEDGMENTS

We thank all members of the Bacterial Cell Biology group (University of Amsterdam) for insightful discussions, and Urša Gubenšek for generating the strain UG10, and Heath Murray (Newcastle University), Pamela Gamba (Newcastle University), Jörg Stülke (University of Göttingen), and Bill Burkholder (Stanford) for providing strains.

This research was funded by EU Marie Curie ITN grants ATP-BCT (020496-2) and AMBER (317338), Marie Curie CIG grant DIVANTI (618452), and a STW Vici grant (12128).

REFERENCES

1. Ainsa JA, Ryding NJ, Hartley N, Findlay KC, Bruton CJ, Chater KF. 2000. WhiA, a protein of unknown function conserved among gram-positive bacteria, is essential for sporulation in *Streptomyces coelicolor* A3(2). J Bacteriol 182:5470–5478. https://doi.org/10.1128/JB.182.19.5470-5478.2000.
2. Flärdh K, Leibovitz E, Buttner MJ, Chater KF. 2000. Generation of a non-sporulating strain of *Streptomyces coelicolor* A3(2) by the manipulation of a developmentally controlled *ftsZ* promoter. Mol Microbiol 38:737–749. https://doi.org/10.1046/j.1365-2958.2000.02177.x.
3. McCormick JR, Flardh K. 2012. Signals and regulators that govern *Streptomyces* development. FEMS Microbiol Rev 36:206–231. https://doi.org/10.1111/j.1574-6976.2011.00317.x.
4. Bush MJ, Bibb MJ, Chandra G, Findlay KC, Buttner MJ. 2013. Genes required for aerial growth, cell division, and chromosome segregation are targets of WhiA before sporulation in Streptomyces venezuelae. mBio 4:e00684-13. https://doi.org/10.1128/mBio.00684-13.
5. Lee D-S, Kim P, Kim E-S, Kim Y, Lee H-S. 2017. Corynebacterium glutamicum WhcD interacts with WhiA to exert a regulatory effect on cell division genes. Antonie Van Leeuwenhoek https://doi.org/10.1007/s10482-017-0953-0.
6. Kaiser BK, Clifton MC, Shen BW, Stoddard BL. 2009. The structure of a bacterial DUF199/WhiA protein: domestication of an invasive endonuclease. Structure 17:1368–1376. https://doi.org/10.1016/j.str.2009.08.008.
7. Surdova K, Gamba P, Claessen D, Siersma T, Jonker MJ, Errington J, Hamoen LW. 2013. The conserved DNA-binding protein WhiA is involved in cell division in *Bacillus subtilis*. J Bacteriol 195:5450–5460. https://doi.org/10.1128/JB.00507-13.
8. Dajkovic A, Pichoff S, Lutkenhaus J, Wirtz D. 2010. Cross-linking FtsZ polymers into coherent Z rings. Mol Microbiol 78:651–668. https://doi.org/10.1111/j.1365-2958.2010.07352.x.
9. Gueiros-Filho FJ, Losick R. 2002. A widely conserved bacterial cell division protein that promotes assembly of the tubulin-like protein FtsZ. Genes Dev 16:2544–2556. https://doi.org/10.1101/gad.1014102.
10. Levin PA, Kurtser IG, Grossman AD. 1999. Identification and characterization of a negative regulator of FtsZ ring formation in *Bacillus subtilis*. Proc Natl Acad Sci U S A 96:9642–9647. https://doi.org/10.1073/pnas.96.17.9642.
11. Haeusser DP, Schwartz RL, Smith AM, Oates ME, Levin PA. 2004. EzrA prevents aberrant cell division by modulating assembly of the cytoskeletal protein FtsZ. Mol Microbiol 52:801–814. https://doi.org/10.1111/j.1365-2958.2004.04016.x.
12. Levin PA, Shim JJ, Grossman AD. 1998. Effect of *minCD* on FtsZ ring position and polar septation in *Bacillus subtilis*. J Bacteriol 180:6048–6051.
13. Bi E, Lutkenhaus J. 1993. Cell division inhibitors SulA and MinCD prevent formation of the FtsZ ring. J Bacteriol 175:1118–1125. https://doi.org/10.1128/jb.175.4.1118-1125.1993.
14. Gregory JA, Becker EC, Pogliano K. 2008. *Bacillus subtilis* MinC destabilizes FtsZ-rings at new cell poles and contributes to the timing of cell division. Genes Dev 22:3475–3488. https://doi.org/10.1101/gad.1732408.
15. Wu LJ, Errington J. 2004. Coordination of cell division and chromosome segregation by a nucleoid occlusion protein in *Bacillus subtilis*. Cell 117:915–925. https://doi.org/10.1016/j.cell.2004.06.002.
16. Adams DW, Wu LJ, Errington J. 2015. Nucleoid occlusion protein Noc recruits DNA to the bacterial cell membrane. EMBO J 34:491–501. https://doi.org/10.15252/embj.201490177.
17. Weart RB, Lee AH, Chien AC, Haeusser DP, Hill NS, Levin PA. 2007. A metabolic sensor governing cell size in bacteria. Cell 130:335–347. https://doi.org/10.1016/j.cell.2007.05.043.
18. Davis NK, Chater KF. 1992. The *Streptomyces coelicolor whiB* gene encodes a small transcription factor-like protein dispensable for growth but essential for sporulation. Mol Gen Genet 232:351–358. https://doi.org/10.1007/BF00266237.
19. Bush MJ, Chandra G, Bibb MJ, Findlay KC, Buttner MJ. 2016. Genome-wide chromatin immunoprecipitation sequencing analysis shows that WhiB is a transcription factor that cocontrols its regulon with WhiA to initiate developmental cell division in *Streptomyces*. mBio 7:e00523-16. https://doi.org/10.1128/mBio.00523-16.
20. Ireton K, Gunther NW, IV, Grossman AD. 1994. *spoOJ* is required for normal chromosome segregation as well as the initiation of sporulation in *Bacillus subtilis*. Microbiology 176:5320–5329.
21. Lee PS, Grossman AD. 2006. The chromosome partitioning proteins Soj (ParA) and Spo0J (ParB) contribute to accurate chromosome partitioning, separation of replicated sister origins, and regulation of replication

initiation in *Bacillus subtilis*. Mol Microbiol 60:853–869. https://doi.org/10.1111/j.1365-2958.2006.05140.x.
22. Sharpe ME, Errington J. 1996. The *Bacillus subtilis soj-spo0J* locus is required for a centromere-like function involved in prespore chromosome partitioning. Mol Microbiol 21:501–509. https://doi.org/10.1111/j.1365-2958.1996.tb02559.x.
23. Sullivan NL, Marquis KA, Rudner DZ. 2009. Recruitment of SMC by ParB-parS organizes the origin region and promotes efficient chromosome segregation. Cell 137:697–707. https://doi.org/10.1016/j.cell.2009.04.044.
24. Gruber S, Errington J. 2009. Recruitment of condensin to replication origin regions by ParB/SpoOJ promotes chromosome segregation in *B. subtilis*. Cell 137:685–696. https://doi.org/10.1016/j.cell.2009.02.035.
25. Ogura Y, Imai Y, Ogasawara N, Moriya S. 2001. Autoregulation of the *dnaA-dnaN* operon and effects of DnaA protein levels on replication initiation in *Bacillus subtilis*. J Bacteriol 183:3833–3841. https://doi.org/10.1128/JB.183.13.3833-3841.2001.
26. Soufo CD, Soufo HJD, Noirot-Gros M-F, Steindorf A, Noirot P, Graumann PL. 2008. Cell-cycle-dependent spatial sequestration of the DnaA replication initiator protein in *Bacillus subtilis*. Dev Cell 15:935–941. https://doi.org/10.1016/j.devcel.2008.09.010.
27. Lemon KP, Kurtser I, Grossman AD. 2001. Effects of replication termination mutants on chromosome partitioning in *Bacillus subtilis*. Proc Natl Acad Sci U S A 98:212–217. https://doi.org/10.1073/pnas.98.1.212.
28. Sahoo T, Mohanty BK, Lobert M, Manna AC, Bastia D. 1995. The contrahelicase activities of the replication terminator proteins of *Escherichia coli* and *Bacillus subtilis* are helicase-specific and impede both helicase translocation and authentic DNA unwinding. J Biol Chem 270:29138–29144. https://doi.org/10.1074/jbc.270.49.29138.
29. Köhler P, Marahiel MA. 1997. Association of the histone-like protein HBsu with the nucleoid of *Bacillus subtilis*. J Bacteriol 179:2060–2064. https://doi.org/10.1128/jb.179.6.2060-2064.1997.
30. Micka B, Groch N, Heinemann U, Marahiel MA. 1991. Molecular cloning, nucleotide sequence, and characterization of the *Bacillus subtilis* gene encoding the DNA-binding protein HBsu. J Bacteriol 173:3191–3198. https://doi.org/10.1128/jb.173.10.3191-3198.1991.
31. Murray H, Errington J. 2008. Dynamic control of the DNA replication initiation protein DnaA by Soj/ParA. Cell 135:74–84. https://doi.org/10.1016/j.cell.2008.07.044.
32. Lemon KP, Grossman AD. 1998. Localization of bacterial DNA polymerase: evidence for a factory model of replication. Science 282:1516–1519. https://doi.org/10.1126/science.282.5393.1516.
33. Meile JC, Wu LJ, Ehrlich SD, Errington J, Noirot P. 2006. Systematic localisation of proteins fused to the green fluorescent protein in *Bacillus subtilis*: identification of new proteins at the DNA replication factory. Proteomics 6:2135–2146. https://doi.org/10.1002/pmic.200500512.
34. Weigel C, Schmidt A, Seitz H, Tungler D, Welzeck M, Messer W. 1999. The N-terminus promotes oligomerization of the *Escherichia coli* initiator protein DnaA. Mol Microbiol 34:53–66. https://doi.org/10.1046/j.1365-2958.1999.01568.x.
35. Messer W, Blaesing F, Jakimowicz D, Krause M, Majka J, Nardmann J, Schaper S, Seitz H, Speck C, Weigel C, Wegrzyn G, Welzeck M, Zakrzewska-Czerwinska J. 2001. Bacterial replication initiator DnaA. Rules for DnaA binding and roles of DnaA in origin unwinding and helicase loading. Biochimie 83:5–12.
36. Leonard AC, Grimwade JE. 2005. Building a bacterial orisome: emergence of new regulatory features for replication origin unwinding. Mol Microbiol 55:978–985. https://doi.org/10.1111/j.1365-2958.2004.04467.x.
37. Leonard TA, Butler PJ, Löwe J. 2005. Bacterial chromosome segregation: structure and DNA binding of the Soj dimer-a conserved biological switch. EMBO J 24:270–282. https://doi.org/10.1038/sj.emboj.7600530.
38. Scholefield G, Whiting R, Errington J, Murray H. 2011. Spo0J regulates the oligomeric state of Soj to trigger its switch from an activator to an inhibitor of DNA replication initiation. Mol Microbiol 79:1089–1100. https://doi.org/10.1111/j.1365-2958.2010.07507.x.
39. Noirot-Gros M-F, Velten M, Yoshimura M, McGovern S, Morimoto T, Ehrlich SD, Ogasawara N, Polard P, Noirot P. 2006. Functional dissection of YabA, a negative regulator of DNA replication initiation in *Bacillus subtilis*. Proc Natl Acad Sci U S A 103:2368–2373. https://doi.org/10.1073/pnas.0506914103.
40. Frees D, Savijoki K, Varmanen P, Ingmer H. 2007. Clp ATPases and ClpP proteolytic complexes regulate vital biological processes in low GC, Gram-positive bacteria. Mol Microbiol 63:1285–1295. https://doi.org/10.1111/j.1365-2958.2007.05598.x.
41. Wiegert T, Homuth G, Versteeg S, Schumann W. 2001. Alkaline shock induces the *Bacillus subtilis* sigma(W) regulon. Mol Microbiol 41:59–71. https://doi.org/10.1046/j.1365-2958.2001.02489.x.
42. Kidane D, Sanchez H, Alonso JC, Graumann PL. 2004. Visualization of DNA double-strand break repair in live bacteria reveals dynamic recruitment of *Bacillus subtilis* RecF, RecO and RecN proteins to distinct sites on the nucleoids. Mol Microbiol 52:1627–1639. https://doi.org/10.1111/j.1365-2958.2004.04102.x.
43. Lesterlin C, Ball G, Schermelleh L, Sherratt DJ. 2014. RecA bundles mediate homology pairing between distant sisters during DNA break repair. Nature 506:249–253. https://doi.org/10.1038/nature12868.
44. Kawai Y, Moriya S, Ogasawara N. 2003. Identification of a protein, YneA, responsible for cell division suppression during the SOS response in *Bacillus subtilis*. Mol Microbiol 47:1113–1122. https://doi.org/10.1046/j.1365-2958.2003.03360.x.
45. Mo AH, Burkholder WF. 2010. YneA, an SOS-induced inhibitor of cell division in *Bacillus subtilis*, is regulated posttranslationally and requires the transmembrane region for activity. J Bacteriol 192:3159–3173. https://doi.org/10.1128/JB.00027-10.
46. Miller MC, Resnick JB, Smith BT, Lovett CM, Jr. 1996. The *Bacillus subtilis dinR* gene codes for the analogue of *Escherichia coli* LexA. Purification and characterization of the DinR protein. J Biol Chem 271:33502–33508.
47. Wang X, Tang OW, Riley EP, Rudner DZ. 2014. The SMC condensin complex is required for origin segregation in *Bacillus subtilis*. Curr Biol 24:287–292. https://doi.org/10.1016/j.cub.2013.11.050.
48. Wang X, Brandao HB, Le TBK, Laub MT, Rudner DZ. 2017. *Bacillus subtilis* SMC complexes juxtapose chromosome arms as they travel from origin to terminus. Science 355:524–527. https://doi.org/10.1126/science.aai8982.
49. Dervyn E, Noirot-Gros M-F, Mervelet P, McGovern S, Ehrlich SD, Polard P, Noirot P. 2004. The bacterial condensin/cohesin-like protein complex acts in DNA repair and regulation of gene expression. Mol Microbiol 51:1629–1640. https://doi.org/10.1111/j.1365-2958.2003.03951.x.
50. Scholefield G, Murray H. 2013. YabA and DnaD inhibit helix assembly of the DNA replication initiation protein DnaA. Mol Microbiol 90:147–159. https://doi.org/10.1111/mmi.12353.
51. Felicori L, Jameson KH, Roblin P, Fogg MJ, Garcia-Garcia T, Ventroux M, Cherrier MV, Bazin A, Noirot P, Wilkinson AJ, Molina F, Terradot L, Noirot-Gros M-F. 2016. Tetramerization and interdomain flexibility of the replication initiation controller YabA enables simultaneous binding to multiple partners. Nucleic Acids Res 44:449–463. https://doi.org/10.1093/nar/gkv1318.
52. Lenhart JS, Sharma A, Hingorani MM, Simmons LA. 2013. DnaN clamp zones provide a platform for spatiotemporal coupling of mismatch detection to DNA replication. Mol Microbiol 87:553–568. https://doi.org/10.1111/mmi.12115.
53. Spizizen J. 1958. Transformation of biochemically deficient strains of *Bacillus subtilis* by deoxyribonucleate. Proc Natl Acad Sci U S A 44:1072–1078. https://doi.org/10.1073/pnas.44.10.1072.
54. Itaya M. 1992. Construction of a novel tetracycline resistance gene cassette useful as a marker on the *Bacillus subtilis* chromosome. Biosci Biotechnol Biochem 56:685–686. https://doi.org/10.1271/bbb.56.685.
55. Morimoto T, Loh PC, Hirai T, Asai K, Kobayashi K, Moriya S, Ogasawara N. 2002. Six GTP-binding proteins of the Era/Obg family are essential for cell growth in Bacillus subtilis. Microbiology 148:3539–3552. https://doi.org/10.1099/00221287-148-11-3539.
56. Lewis PJ, Marston AL. 1999. GFP vectors for controlled expression and dual labelling of protein fusions in *Bacillus subtilis*. Gene 227:101–110. https://doi.org/10.1016/S0378-1119(98)00580-0.
57. Gamba P, Jonker MJ, Hamoen LW. 2015. A novel feedback loop that controls bimodal expression of genetic competence. PLoS Genet 11:1–32. https://doi.org/10.1371/journal.pgen.1005047.
58. Gibson DG, Young L, Chuang R, Venter JC, Hutchison CA, III, Smith HO. 2009. Enzymatic assembly of DNA molecules up to several hundred kilobases. Nat Methods 6:343–345. https://doi.org/10.1038/nmeth.1318.
59. Hamoen LW, Smits WK, de Jong A, Holsappel S, Kuipers OP. 2002. Improving the predictive value of the competence transcription factor (ComK) binding site in *Bacillus subtilis* using a genomic approach. Nucleic Acids Res 30:5517–5528. https://doi.org/10.1093/nar/gkf698.
60. Homer N. 2010. TMAP: the Torrent Mapping Program.
61. Li H, Durbin R. 2009. Fast and accurate short read alignment with Burrows-Wheeler transform. Bioinformatics 25:1754–1760. https://doi.org/10.1093/bioinformatics/btp324.
62. Li H, Durbin R. 2010. Fast and accurate long-read alignment with

Burrows-Wheeler transform. Bioinformatics 26:589–595. https://doi.org/10.1093/bioinformatics/btp698.
63. Ning Z, Cox AJ, Mullikin JC. 2001. SSAHA: a fast search method for large DNA databases. Genome Res 11:1725–1729. https://doi.org/10.1101/gr.194201.
64. Anders S, Pyl PT, Huber W. 2015. HTSeq–a Python framework to work with high-throughput sequencing data. Bioinformatics 31:166–169. https://doi.org/10.1093/bioinformatics/btu638.
65. Love MI, Huber W, Anders S. 2014. Moderated estimation of fold change and dispersion for RNA-seq data with DESeq2. Genome Biol 15:550. https://doi.org/10.1186/s13059-014-0550-8.
66. Daniel RA, Williams AM, Errington J. 1996. A complex four-gene operon containing essential cell division gene *pbpB* in *Bacillus subtilis*. J Bacteriol 178:2343–2350. https://doi.org/10.1128/jb.178.8.2343-2350.1996.
67. Miller J. 1972. Experiments in molecular genetics. Cold Spring Harbor Laboratory Press, Cold Spring Harbor, NY.